CO$_2$ Fixation by Dimeric Tb(III) Complexes: Synthesis, Structure, and Magnetism

Malay Dolai,* Surajit Biswas, Eufemio Moreno-Pineda,* Wolfgang Wernsdorfer, Mahammad Ali,* Razan A. Alshgari, Saikh Md. Wabaidur, and Ashutosh Ghosh*

ABSTRACT: Two dinuclear complexes, $[Tb_2(L^1)_2(piv)_2(NO_3)_2]\cdot H_2O$ (**1**) and $[Tb_2(L^2)_2(CF_3CO_2)_2(H_2O)_4].2NO_3$ (**2**), have been prepared and characterized by single-crystal X-ray diffraction, where each metal ion is doubly phenoxido-bridged by the two phenolato oxygen atoms of the tetradentate Schiff-base ligand. Previous magnetic studies of **1** show that it is not a single-molecule magnet (SMM), while AC magnetic measurements of **2** show that it relaxes quite fast with μSQUID measurements revealing the presence of an interaction operating between the Tb ions. Through DC, μSQUID, and CASSCF calculations, the strength of the interaction in **2** can be quantified, which is of dipolar origin. Both complexes showed efficient catalytic activity toward the carbon dioxide insertion reaction into epoxides for the formation of organic cyclic carbonates. Catalytic synthesis of

organic cyclic carbonates smoothly occurred at 60 °C under 1 bar carbon dioxide pressure and neat conditions. Exocyclic as well as endocyclic epoxides produced a respective cyclic carbonate product with moderate to high yield (43−100%). Moreover, a high turnover number (7300−10000) along with a high turnover frequency (537.5−5000 h^{-1}) are found in this catalytic reaction.
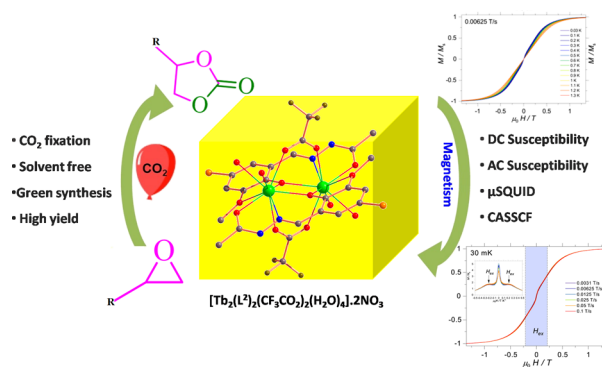
INTRODUCTION

Due to the excessive use of fossil fuels, the concentration of atmospheric carbon dioxide (CO$_2$) has reached values resulting in global warming. Global warming produces various serious environmental threats such as unpredictable climate change, the melting of glaciers, and increments of sea levels.[1] To decrease the constantly increasing CO$_2$ levels, capture, storage and utilization of CO$_2$ become more and more essential. Since CO$_2$ also represents a cheap, abundant, renewable, nonhazardous C1-feedstock,[2−5] chemical fixation of carbon dioxide has prospective economical benefits as it produces numerous highly valuable chemicals.[6−8] In this context, coupling between carbon dioxide and epoxides for the synthesis of organic cyclic carbonates is the most common CO$_2$ fixation reaction. This reaction is biocompatible and ecofriendly and represents a 100% atom efficiency.[9] Moreover, the organic cyclic carbonates have immense applications in diverse fields such as electrolytes of batteries, intermediates of fine chemical/pharmaceuticals, engineering plastic syntheses, polymer production, aprotic green polar solvents, etc.[10−16] There are several catalysts being developed for the preparation of cyclic carbonate from epoxides and carbon dioxide such as transition-metal-based catalysts (like Co,[17,18] Cr,[19−21] Fe,[22−27] and Zn[28−32]), main-group metal

complex catalysts (like Li,[33] Al,[34−37] Mg,[38,39] and Ca[40,41]), and organocatalysts.[42−47]

In cycloaddition of CO$_2$ into epoxides, generally a Lewis acidic site is necessary for the activation of epoxides. Mainly vacant coordination sites of metal nodes fulfill these criteria. The trivalent lanthanide ions (Ln^{III}) can be expedient for this purpose due to their higher Lewis acidic and oxophilic nature.[48,49] The oxophilic nature of lanthanides frequently eases the small solvent molecules' coordination which can be smoothly disconnected to make vacant coordination sites. Moreover, the strong Ln^{III}−O bond should promote the communication with epoxides to encourage the ring opening and robustness of the molecules upon chemical and thermal exposure. $[\{Ln^{III}(BTB)(H_2O)\}\cdot H_2O]_n$ [Ln^{III} = Gd^{III}, Sm^{III}; BTB = 1,3,5-tris (4-carboxy phenyl) benzene)],[50] Gd-pyromellitic dianhydride,[51] $[(CH_3)_2NH_2][Ln^{III}_3(OH)$-

$(NDC)_3(HCOO)_3]$, and $[(CH_3)_2NH_2][Ln^{III}_3(OH)$-$(BDC)_3(HCOO)_3]$ $(Ln^{III} = Er^{III}, Tb^{III}; NDC = 1,4$-napthalenedicarboxylate; BDC = 1,4-benzenedicarboxylate)[52] are a few example of lanthanides acting as catalysts. The existences of Lewis acidic and basic motifs within the ligand framework which are design for complexation with lanthanides also have importance for the enhancement of the catalytic efficacy for the cyclization reaction, as the presence of a Lewis basic center with the close vicinity of a Lewis acidic center facilitates the fixation of CO_2 in the target substrate. Few previous reports based on the above tactic involve $[Zn_{3.5}(PDC)_2(H_2O)_{10}]$, where a lone pair electron in the N atom of 1,1′-(propane-1,3-diyl)bis(1H-pyrazole-3,5-dicarboxylic acid) (PDC)[53] acts as a Lewis base, and $\{[(CH_3)_2NH_2]$-$[Zn^{II}Tb^{III}(TDP)(H_2O)]\cdot3DMF\cdot3H_2O\}_n$, where uncoordinated carboxylate-O atoms functioned as a Lewis base.[54]

Furthermore, in recent years, lanthanide (4f) ion-based complexes have displayed fascinating properties, leading to their proposal in several technological applications.[55,56] 4f complexes are particularly interesting due to their magnetic properties, such as the existence of an energy barrier to the reversal of the magnetization, leading to the so-called single-molecule magnet (SMM) behavior.[57] Furthermore, multifunctional molecular materials have attracted attention due to the possibility to exploit different cooperative physical properties in a single entity. In this regard, 4f-SMMs have been shown to possess two or more physical properties[58−63] allowing even the observation of cooperative effects.[61]
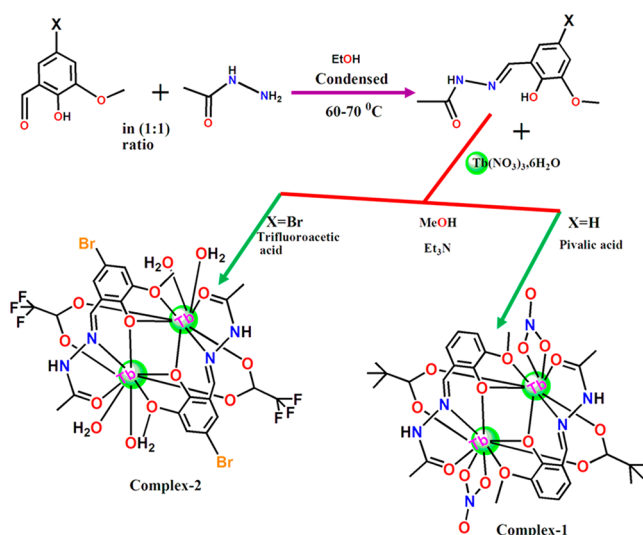
With this in mind, several strategies have been employed by synthetic chemists to produce these materials. The choice of a proper ligand plays a crucial role not only in dinuclear complex formation but also in promoting exchange interactions between the spin centers. In order to obtain a high-performance catalyst, the above strategies were considered, and two multidentate ligands, N'-(2-hydroxy-3-methoxybenzylidene) acetohydrazide (HL^1) and N'-(2-hydroxy-3-methoxy-5-bromo benzylidene) acetohydrazide (HL^2), were employed for the synthesis of $[Tb_2(L^1)_2(piv)_2(NO_3)_2]\cdot H_2O$ (1) and $[Tb_2(L^2)_2(CF_3CO_2)_2(H_2O)_4]\cdot2NO_3$ (2), respectively. In both cases, the uncoordinated −NH group of each ligand provides a free lone pair for the transfixation of CO_2 molecules. $[Tb_2(L^1)_2(piv)_2(NO_3)_2]\cdot H_2O$ (1) and $[Tb_2(L^2)_2(CF_3CO_2)_2(H_2O)_4]\cdot2NO_3$ (2) act as efficient catalysts in cycloaddition of carbon dioxide with epoxides at room temperature under 1 bar CO_2 pressure and neat conditions. Hence, the syntheses, structure, and magnetic and catalytic properties of 1 and 2 are discussed herein.

RESULTS AND DISCUSSION

Synthesis Procedure. Tetradentate Schiff base ligands (HL^1 and HL^2) were prepared according to the reported procedure.[64] The ligands HL^1 and HL^2, respectively, were combined with $Tb(NO_3)_3\cdot6H_2O$ and pivalic acid/trifluoroacetic acid and triethylamine yielding $[Tb_2(L^1)_2(piv)_2(NO_3)_2]\cdot$$H_2O$ (1) and $[Tb_2(L^2)_2(CF_3CO_2)_2(H_2O)_4]\cdot2NO_3$ (2) (Scheme 1). More details are given in the Supporting Information.

Structural Description. The crystal structure analysis shows that complexes 1 and 2 crystallized in the *monoclinic* and *trigonal* system with the space group $P2_1/n$ and $R\bar{3}$ for 1 and 2, respectively. The crystal structure for 1 has been previously reported;[64] hence, just a detailed description for 2 is given below.

Scheme 1. Synthesis of the Ligands (Top) and Syntheses of Complexes 1 and 2 (Bottom)

The asymmetric unit of complex 2 contains one-half of the total molecule, that is, $[TbL^2(CF_3COO\text{-}\eta O)(O1w,O2w\text{-}\eta O)]$ for 2 (Figure 1a). The complexes are neutral and possess a similar structural topology. The side and top views of the molecular structure of 2 are depicted in Figure 1b,c, which clearly demonstrate that the complex is a dinuclear $\{Tb^{III}\}_2$ species where each metal atom is doubly phenoxido-bridged by the two phenolato oxygen atoms of the ligand. The dinuclear complex was assembled with the help of two monodeprotonated ligands. Each ligand bounds the metal in its keto form, and four coordination sites are used for binding the metal centers. The phenolate oxygen atom behaves as a bridging ligand between the two terbium(III) centers. Hence, the overall coordination behavior from each ligand is $\mu_4\text{-}\eta^1:\eta^2:\eta^1:\eta^1$.[64] The phenolato oxygen bridging results in the formation of a four-membered Tb_2O_2 motif (Figure S1a). The Tb−Tb distance within the four-membered ring is 3.691 Å with a Tb−O−Tb angle of 103.73° for 2. Further, the dinuclear complex is chelated by the coordination action of two trifluoro-acetate and four water solvents. Thus, both of the Tb^{III} are nine-coordinated, are surrounded by an identical coordination environment (O8N), and possess the distorted monocapped square-antiprism geometry (Figure S1b). The Tb−$O_{hydrazone}$ bond distances are 2.357 Å which is very similar to those in other previous work for a keto group involved in binding. The rest of the Tb−O bond lengths are in the range 2.333−2.631 Å for 2; that is, Tb−O bond lengths for 2 are greater than for complex 1.[64]

The selected bond lengths and bond angles around metal centers in 2 are given in Tables S1−S3. Upon inspection of H-bonding and molecular assemblies on 2, dinuclear units are interconnected through hydrogen bonding interactions between the hydrazone H and O of the nitrate counteranion (N2−H2N···O8, 2.110 Å) and between the coordinated water molecules and O of nitrate (O8···H7b−O7, 2.064 Å; and O6−H6b···O9, 2.127 Å; Figure 1d), simultaneously acting as templates for an exclusive honeycomb network. The honeycomb layers of the chelated dinuclear units occupy the vacant space between successive counteranion and dinuclear unit layers leading to interpenetration of a 3D hydrogen-bonded network (Figure 1e). However, the displacement of Tb^{III} from the corresponding least-squares $\{O(phenoxido)_2O(methoxy)_2\}$
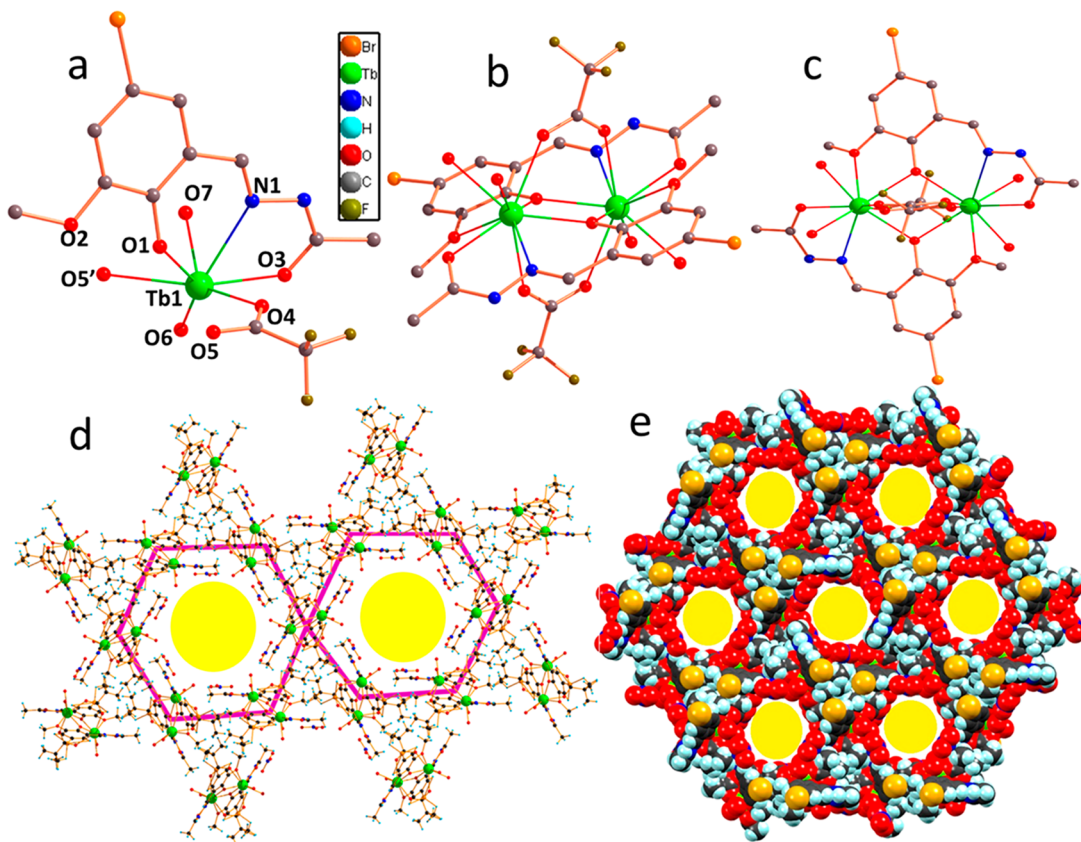
Figure 1. (a) Asymmetric unit of **2**. (b) Side and (c) top view of the crystal structure of **2**. (d) Motif of honeycomb and (e) supramolecular H-bonded 3D network with honeycomb architecture in packing diagram of **2**.
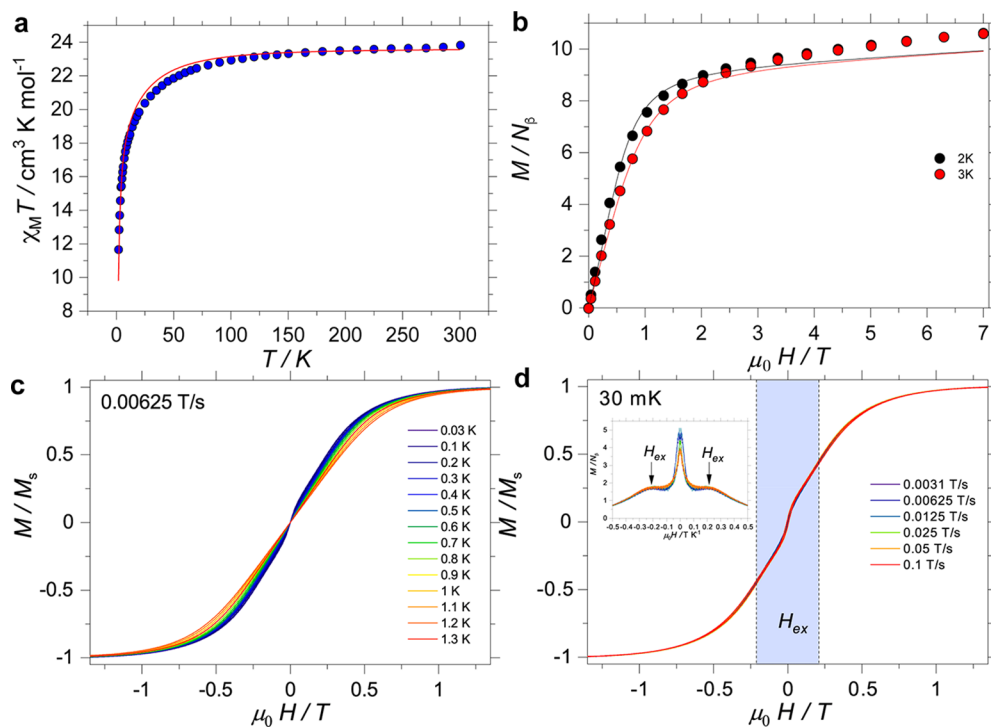

Figure 2. (a) $\chi_M(T)$ for **2** with $H_{dc} = 1000$ G and in the temperature range from 2.0 to 300.0 K. (b) $M(H)$ curves in the field range of 0 and 7 T at 2 and 3 K. Solid traces in panels a and b are fits employing CF parameters from CASSCF calculations and the Lines model (eq 1). (c) Temperature-dependent μSQUID loops with a sweep rate of 0.00625 T/s. (d) Sweep-rate dependence of the μSQUID loops at 30 mK. The inset and dotted lines show the inflection point corresponding to the exchange field between the Tb^{3+} ions.
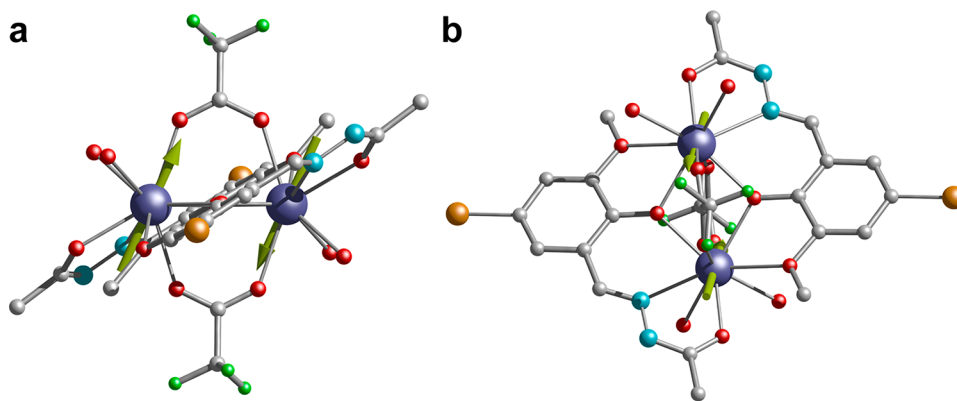
Figure 3. (a) Side and (b) top view of the crystal structure of the $[Tb_2(L^2)_2(CF_3CO_2)_2(H_2O)_4]\cdot 2NO_3$ complex (**2**). The green arrow represents the anisotropic easy axes obtained from CASSCF calculation. Color code: Tb, blue; N, cyan; F, bright green; O, red; C, gray. Hydrogens were omitted for clarity.

planes is 0.926 Å for **2**, suggesting that the Tb^{III} ion lies significantly away from the concerned mean plane.

MAGNETIC CHARACTERIZATION

The magnetic characteristic of **1** has been previously described;[64] hence, we just provide the magnetic description of **2**. Direct current (DC) susceptibility measurements of **2** were carried out in the temperature range from 2 to 300 K in a field of 1000 Oe. The experimental $\chi_M T$ value at room temperature of 23.48 cm^3 mol^{-1} K is close to the expected value of 23.63 cm^3 mol^{-1} K for two free Tb^{3+} ions (Figure 2a). The $\chi_M T$ values gradually reduce with decreasing temperature and reach a value of 9.76 cm^3 mol^{-1} K at 2.0 K. The downturn shown in the $\chi_M T$ behavior of **2** could be a consequence of depopulation of the Stark levels and/or magnetic interaction occurring between the Tb^{3+} ions. The field dependence of the magnetization of compounds **2** was measured and is shown in the Supporting Information (Figure 2b). At a DC field of 7 T and 2 K, a value of 9.6 Nβ for **2** was obtained. The lack of saturation of magnetization, the non-superposition of the reduced magnetization data (M vs H/T) at high fields, and the rapid increase of M at low fields suggest the presence of low-lying excited states and/or significant magnetic anisotropy. An alternating current (AC) magnetic susceptibility measurement for **2** was also carried out at zero and different applied DC fields. Although some out-of-phase of the magnetic susceptibility was detected, no clear maximum was observed in the frequency and temperature range, indicating fast relaxation in the system (see Figure S7).

To confirm whether **2** is an SMM, μSQUID measurements were conducted in a single crystal of the dimeric terbium complex. The hysteresis curves are narrow and do not show the temperature- and sweep-rate-dependent behavior characteristic of SMMs, confirming the fast relaxation characteristics of **2** (Figure 2c,d). Additionally, μSQUID measurements allow the evaluation of the interaction occurring between the Tb^{3+} centers. A close inspection of the loops at the lowest temperature and different sweep rates shows a small interaction, as revealed by the inflection points between ± 0.21 T (Figure 2d).[65−67] The value of the magnetic field at the crossing at ± 0.21 T allows the direct calculation of the exchange coupling J_{ex} between the two Tb^{3+} ions through Hex = $-2J_{ex}m_J/g_J\mu_\beta$, where $m_J = 6$, $g_J = 3/2$, μ_β is the Bohr magneton, and with the two Tb^{3+} ions having parallel easy axes. J_{ex} is found to be -0.012 cm^{-1} (18 mK), which corresponds to a purely dipolar interaction.

To rationalize the magnetic properties of **2**, CASSCF calculations were performed employing *OpenMolcas*[68] and the experimental crystal structure of **2** (see Figure 3). The single ion magnetic properties show a highly axial Ising character of the uncoupled ions, with $g_x = g_y \approx 0$ and $g_z \approx 18$, with the first excited state lying at ~100 cm^{-1}; however, inspection of the transition matrix elements shows that relaxation is quite effective in **2**, indicating that, in this scenario, where no interaction between the Tb^{3+} ions is present, **2** would have behaved as a modest SMM. In contrast, no clear SMM behavior was observed for **2**, while DC and μSQUID studies show that the Tb^{3+} ions interact through dipolar fields. The dipolar interaction effectively couples the magnetic moments of both Tb^{3+} ions, inducing new effective relaxation pathways in **2** and, hence, inducing fast relaxation. Note that relaxation is quite effective for the isolated Tb^{3+} ions; thus, the interaction between the Tb^{3+} ions accelerates the dynamics of the system. Employing the crystal field parameters obtained from CASSCF calculations, and the Lines model,[69,70] which utilizes an isotropic exchange between the spin component of the angular momenta ($S = 5/2$ for Tb^{3+}), it is possible to reproduce the $\chi_M T(T)$ and $M(H)$ for **2** (see Figure 2a) with $J_{Lines} = -0.042$ cm^{-1} (59 mK) and Hamiltonian of the form:

$$\mathcal{H}^i_{Dy} = \mathcal{H}^i_{lf} + g_J\mu_0\mu_B \mathbf{J}^i_{Lines}\cdot\mathbf{H}_z \qquad (1)$$

where $H^i_{lf} = \sum_{k,-k\leq q\leq q} u_k B_k^q O_k^q$ is the ligand field Hamiltonian expressed in Steven's operator with u_i the Stevens factor, O_k^q the Stevens operator, and B_k^q the ligand field parameters obtained from CASSCF calculations. Note that although a good agreement for the $\chi_M T(T)$ and $M(H)$ was found, the exchange value obtained from the Lines analysis is not directly comparable to the experimental exchange value obtained from μSQUID loops.

CATALYTIC ACTIVITY

Catalytic activities of synthesized lanthanide complexes (**1** and **2**) were performed in the addition reaction of carbon dioxide and epoxides for the formation of organic carbonates. Some controlled reactions were carried out in order to optimize the catalytic reaction conditions by taking substrate 2-(chloromethyl) oxirane under 1 atm CO$_2$ pressure at room temperature in the presence of complex **1** or **2** as catalyst. The reaction of 2-(chloromethyl)oxirane (12 mmol) and carbon dioxide under precise conditions in the presence of **1** as catalyst and

tetrabutylammonium bromide (TBAB) as cocatalyst therefore produced 71% of the desired 4-(chloromethyl)-1,3-dioxolan-2-one as product after 2 h (Table 1, entry 1). The same reaction

Table 1. Parameter Optimization for Catalytic 4-(Chloromethyl)-1,3-dioxolan-2-one Synthesis via Addition of CO_2 and 2-(Chloromethyl)oxirane[a]

entry	catalyst	cocatalyst	time (h)	yield[b] (%)
1	**1**	TBAB	2	71
2	**2**	TBAB	2	76
3	**1**		2	trace
4	**2**		2	trace
5		TBAB	2	14
6	**1**	TBAI	2	57
7	**1**	TBAC	2	44
8	**1**	NaCl	2	11
9	**1**	KI	2	13
10	**1**	KBr	2	17
11	**HL¹**	TBAB	2	16
12	**HL²**	TBAB	2	18
13	$Tb(NO_3)_3 \cdot 6H_2O$	TBAB	2	15

[a]Reaction conditions: 2-(chloromethyl)oxirane (12 mmol), catalyst (0.01 mol %), cocatalyst (0.8 mol %), carbon dioxide balloon, room temperature. [b]Gas chromatography yield.

gave 76% of desired carbonate product after 2 h in the presence of catalyst **2** (Table 1, entry 2). When both reactions were executed in the absence of cocatalyst TBAB, then only a trace amount of corresponding product was obtained (Table 1, entries 3 and 4). Again, an identical reaction performed in the presence of TBAB but in the absence of any catalyst yielded 14% of 4-(chloromethyl)-1,3-dioxolan-2-one (Table 1, entry 5). Basically, the metal center Tb of complexes **1** and **2** as the Lewis acidic center only activated the epoxide substrate, but ring opening of activated epoxide occurs through the nucleophilic attack of Br^- ions (dissociated from TBAB). Thus, the smooth production of organic carbonate by the addition reaction of epoxide and CO_2 is the outcome of the synergistic effect of catalyst and cocatalyst TBAB.[71] The cocatalyst screening was further optimized by using various inorganic salts such as sodium chloride (NaCl), potassium iodide (KI), and potassium

bromide (KBr) and organic salts like TBAI (tetrabutylammonium iodide) and TBAC (tetrabutylammonium chloride) in this reaction (Table 1, entries 6−10). It was observed that our synthesized lanthanide-based catalysts in conjunction with TBAB have an utmost synergistic effect toward the organic carbonate synthetic reaction. This is because of the higher nucleophilicity of Br^- than I^- as well as the improved leaving capability in comparison to Cl^-.[72]

The ligands **HL¹** and **HL²** were used as catalyst instead of two complexes along with TBAB in two different reaction setups (Table 1, entries 11 and 12). Again, the lanthanide precursor $Tb(NO_3)_3 \cdot 6H_2O$ was also used as catalyst for the same reaction (Table 1, entry 13). In each of these three cases, the obtained results are almost similar with the result when only TBAB was used in the reaction. Thus, it is significant to point out that terbium metal within both **HL¹** and **HL²** ligand environments with TBAB efficiently executes the catalytic reaction.

After the selection of cocatalyst for the catalytic reaction, reaction temperature and duration were optimized. From Figure 4a, it is clear that, with the rising reaction temperature, the yield percentage of 4-(chloromethyl)-1,3-dioxolan-2-one also rises, and it reaches a maximum (i.e., 100%) at 60 °C (Figure 4a). An increment in the reaction temperature causes a greater number of collisions between the active sites of catalyst and substrate, and as a result, the yield product is enhanced. The kinetics of this catalytic reaction was monitored, and the results are plotted in Figure 4b. A lower yield of the desired product was found when the catalytic reaction was monitored in the presence of a lower amount of catalyst **1** (0.008 mol %) at 60 °C.

Exocyclic as well as endocyclic epoxides were produced in moderate to high yield for corresponding carbonate products under optimized reaction conditions. 2-(Chloromethyl)oxirane was fully converted into its corresponding carbonates in a very short reaction duration (2 h), whereas other terminal epoxides required relatively more time to produce a high percentage of carbonate product (Table 2, entries 1−8). This is due to the presence of an electron-withdrawing chloro group in 2-(chloromethyl)oxirane making the C−O bond cleavage faster. Further, the side chain of terminal epoxides was increased, and then, the reaction rate was slowed down due to the steric hindrance, causing the production with a relatively lower yield (Table 2, entries 5−8). Styrene oxide and phenyl glycidyl ether produced the respective carbonates in a very good quantity yield (73−81%) after 4−5 h of reaction (Table 2, entries 9−12). Endocyclic epoxide (i.e., cyclohexene oxide) requires a longer
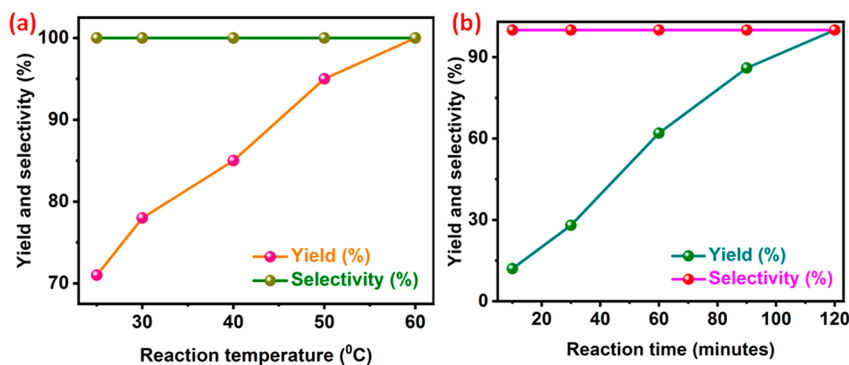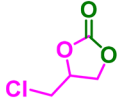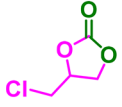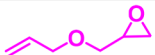

Figure 4. (a) Optimization of reaction temperature [conditions: 2-(chloromethyl) oxirane (12 mmol), **1** (0.01 mol %), TBAB (0.8 mol %), carbon dioxide balloon, 2 h] and (b) kinetics of catalytic reaction [conditions: 2-(chloromethyl) oxirane (12 mmol), **1** (0.01 mol %), TBAB (0.8 mol %), carbon dioxide balloon, 60 °C].

Table 2. Catalytic Addition of CO$_2$ into Epoxides[a]

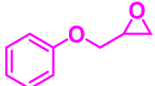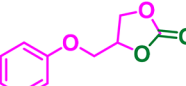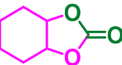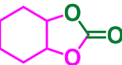| Entry	Catalyst	Epoxides	Product	Time (h)	% of GC yield (% Selectivity) [isolated yield %]	TON[b]	TOF[bc] (h^{-1})
1	1			2	100 (100)[97]	10000	5000.0
2	2			2	100 (100)[97]	10000	5000.0
3	1			2.5	100 (100)[96.5]	10000	4000.0
4	2			2.5	100 (100)[96]	10000	4000.0
5	1			3	94 (100)[91.5]	9400	3133.3
6	2			3	97 (100)[93]	9700	3233.3
7	1			3	90 (100)[87]	9000	3000.0
8	2			3	93 (100)[90.5]	93000	3100.0
9	1			5	73 (100)[66]	7300	1460.0
10	2			5	78 (100) [75]	7800	1560.0
11	1			4	75 (100)[72.5]	7500	1875.0
12	2			4	81 (100) [77]	8100	2025.0
13	1			8	43 (100) [40]	4300	537.5
14	2			8	48 (100) [45]	4800	600.0
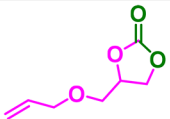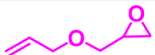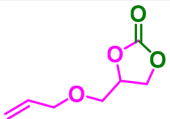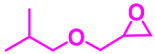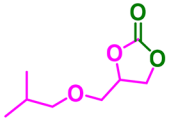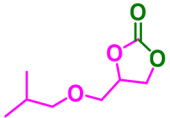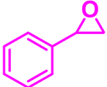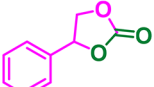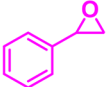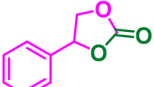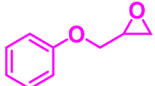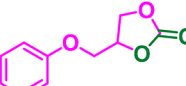
[a]Reaction conditions: epoxides (12 mmol), catalyst (0.01 mol %), TBAB (0.8 mol %), 60 °C, carbon dioxide balloon, neat conditions. [b]TON (turnover number): number of moles of product formed per mole of catalyst. [c]TOF (turnover frequency): number of moles of formed produced per mole of catalyst/time (in h).

Table 3. Comparison of Our Synthesized Catalyst with Previously Reported Lanthanide Metal-Based Catalyst for 4-(Chloromethyl)-1,3-dioxolan-2-one Synthesis via Catalytic Addition Reaction of 2-(Chloromethyl)oxirane and Carbon Dioxide

catalyst	cocatalyst	reaction conditions	yield (%)	TON[a]/TOF[b] (h^{-1})	ref
[Ln(μ-L)(μ_3-L)(H$_2$O)]$_n$X$_n$][a] (0.1 mol %)	TBAB (0.75 mol %)	epoxide (10 mmol), 120 °C, 10 bar CO$_2$, 3 h	98	981/327	73
[L$_2$La$_2$(THF)$_4$(4$^{L^a}$)][b] (0.2 mol %)	TBAB (0.4 mol %)	epoxide (10 mmol), 100 °C, 1 bar CO$_2$, 18 h	95		74
C$_{55}$H$_{88}$LaN$_2$O$_4$ (0.3 mol %)	TBAI (0.6 mol %)	epoxide (3 mmol), 25 °C, 1 bar CO$_2$, 24 h	91		75
[Sm$_4$L$_6$(NO$_3$)$_4$)·4(MeCN))][c] (0.01 mol %)	TBAB (0.75 mol %)	epoxide (10 mmol), 120 °C, 1 MPa CO$_2$, 1.5 h	99	10050/6700	76
[Ln$_2$(ImBDC)$_3$(2H$_2$O)]$_n$[d] (0.2 mol %)	TBAB (2.5 mol %)	epoxide (10 mmol), 80 °C, 0.1 MPa CO$_2$, 9 h	>99	995/110.5	77
[Eu^{III}(Habtc)(H$_2$O)$_2$]·2H$_2$O[e] (0.031 mol %)	TBAB (0.5 mol %)	epoxide (20 mmol), 80 °C, 1 bar CO$_2$, 4 h	92	2778/694	78
[H$_2$LSmCl$_2$·THF][f] (0.02 mmol)	TBAB (0.04 mmol)	epoxide (2 mmol), 70 °C, 0.1 MPa CO$_2$, 24 h	99		79
[La$_2$(HL)$_2$(H$_2$L)(NO$_3$)(CH$_3$OH)(H$_2$O)][g] (0.05 mol %)	TBAB (0.75 mol %)	epoxide (10 mmol), 120 °C, 8 bar CO$_2$, 2 h	94	1920/960	80
1 (0.01 mol %)	TBAB (0.8 mol %)	epoxide (12 mmol), 60 °C, 1 bar CO$_2$, 2 h	100	10000/5000.0	this work
2 (0.01 mol %)	TBAB (0.8 mol %)	epoxide (12 mmol), 60 °C, 1 bar CO$_2$, 2 h	100	10000/5000.0	this work

[a]L = 1,3-bis(4-carboxyphenyl) imidazolium carboxylate(1+), Ln = Yb, X = Br. [b]La = N,N-bis(2-hydroxy-3,5-di-tert-buthylbenzyl)-2-aminoethanol. [c]L = Schiff base between 5-allyl-2-hydroxy-3-methoxy benzohydrazide and 4-(diethylamino)-2-hydroxybenzaldehyde. [d]ImBDC = 2-(imidazol-1-yl)terephthalic acid), Ln = Tb. [e]H$_4$abtc = 3,3,5,5-azobenzenetetracarboxylic acid. [f]H$_2$L = (S)-2,4-di-tert-butyl-6-[[2-(hydroxydiphenylmethyl)-pyrrolidinlyl]methyl]pheno. [g]H$_3$L = Shiff base between 2-hydroxy-3-(hydroxymethyl)-5-methylbenzaldehyde and isoniazid.

reaction duration (8 h) to produce a moderate yield (43–48%) of carbonate through this catalytic addition reaction (Table 2, entries 13 and 14).

A literature survey for a comparison of 4-(chloromethyl)-1,3-dioxolan-2-one synthesis via catalytic addition reaction of 2-(chloromethyl)oxirane and carbon dioxide in the presence of lanthanide-based metal catalysts is given in Table 3. Three previously published reports[73−80] showed that a very high yield of 4-(chloromethyl)-1,3-dioxolan-2-one (94−99%) was produced under neat reaction conditions and high CO_2 pressure (≥8 bar). A few other reported methodologies[74,75,77−79] produced a high percentage of desired product under 1 bar CO_2 pressure in the presence of cocatalyst after ≥4 h of reaction. In this report, a high quantity of carbonate product is formed under 1 bar CO_2 pressure in just a 2 h reaction interval. Again, high TON and TOF are observed in this catalytic reaction.

CATALYTIC REACTION MECHANISM

The mechanism for the catalytic synthesis of cyclic carbonates by cycloaddition of CO_2 into epoxides in the presence of TBAB is depicted in Figure 5 on the basis of previously published
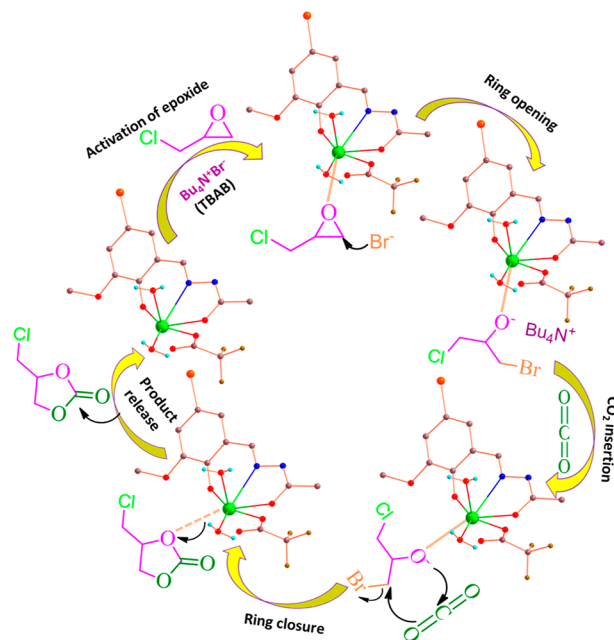

Figure 5. Probable mechanistic pathway for the catalytic cycloaddition of CO_2 with epoxides in the presence of Tb_2 complex (asymmetric unit is shown for clarity).

articles.[73−80] At first, epoxide is activated by the terbium(III) center of complex **1** or **2** and produces a terbium activated epoxide intermediate. Then, nucleophilic attack of $Br^−$ of tetrabutylammonium bromide causes the ring-opening of the terbium(III) activated epoxide intermediate in order to form Tb-bonded bromo-alkoxide. Thereafter, nucleophilic attack of the Tb-bonded bromo-alkoxide in carbon dioxide generates a Tb-carbonate intermediate. Finally, ring closure occurs to release cyclic carbonate, catalyst, and bromide for the next catalytic cycle.[75] We have framed the mechanism by using the asymmetric unit for clarity. However, we can suppose that the dimeric unit with two metal centers may give a higher yield of the final product as cyclic carbonates.

CONCLUSION

Two terbium(III) binuclear complexes based on two tetradentate Schiff-base ligands were synthesized and structurally characterized through single-crystal XRD. The complex **2** exhibited a hydrogen-bonded honeycomb structure. The standard magnetic measurements showed that **1** is not an SMM, as reported in a previous article,[64] whereas complex **2** has a fast relaxation with μSQUID measurements and is supported by CASSCF calculations. Besides, complexes **1** and **2** acted as efficient catalysts for the synthesis of organic cyclic carbonates via the addition reaction of carbon dioxide and epoxides. The efficiency of the catalysis of these complexes was compared with previous reports[73−80] in tabulated form. Hence, it is observed that the moderate to very good yield of carbonate products with high TON/TOF values is achieved by this catalytic reaction (using complexes **1** and **2** as catalysts) at 60 °C under 1 bar CO_2 pressure and solvent-free conditions from terminal and internal epoxides.

AUTHOR INFORMATION

Corresponding Authors

Malay Dolai − *Department of Chemistry, University College of Science, University of Calcutta, Kolkata 700 009, India; Department of Chemistry, Prabhat Kumar College, Purba Medinipur 721404 West Bengal, India; Department of Chemistry, Jadavpur University, Kolkata 700 032 West Bengal, India;* orcid.org/0000-0001-7697-3376; Email: dolaimalay@yahoo.in

Eufemio Moreno-Pineda − *Departamento de Química-Física, Escuela de Química, Facultad de Ciencias Naturales, Exactas y Tecnología, Universidad de Panamá, Transístmica 0874, Panamá;* orcid.org/0000-0002-9643-0341; Email: Eufemio.moreno@up.ac.pa

Mahammad Ali − *Department of Chemistry, Jadavpur University, Kolkata 700 032 West Bengal, India;* orcid.org/0000-0003-0756-0468; Email: m_ali2062@yahoo.com

Ashutosh Ghosh − *Department of Chemistry, University College of Science, University of Calcutta, Kolkata 700 009, India;* orcid.org/0000-0003-2026-7565; Email: ghosh_59@yahoo.com

Authors

Surajit Biswas − *Department of Chemistry, Jadavpur University, Kolkata 700 032 West Bengal, India*

Wolfgang Wernsdorfer − *Institute for Quantum Materials and Technology (IQMT), Karlsruhe Institute of Technology (KIT), D-76344 Eggenstein-Leopoldshafen, Germany; Physikalisches Institut, Karlsruhe Institute of Technology, D-76131 Karlsruhe, Germany;* orcid.org/0000-0003-4602-5257

Razan A. Alshgari − *Department of Chemistry, College of Science, King Saud University, Riyadh 11451, Saudi Arabia*

Saikh Md. Wabaidur − *Department of Chemistry, College of Science, King Saud University, Riyadh 11451, Saudi Arabia*

Notes

The authors declare no competing financial interest.

REFERENCES

(1) Otto, A.; Grube, T.; Schiebahn, S.; Stolten, D. Closing the loop: captured CO2 as a feedstock in the chemical industry. *Energy Environ. Sci.* **2015**, *8*, 3283−3297.

(2) Song, Q.-W.; Zhou, Z.-H.; He, L.-N. Efficient, selective and sustainable catalysis of carbon dioxide. *Green Chem.* **2017**, *19*, 3707−3728.

(3) Dabral, S.; Schau, T. The Use of Carbon Dioxide (CO_2) as a Building Block in Organic Synthesis from an Industrial Perspective. *Adv. Synth. Catal.* **2019**, *361*, 223−246.

(4) Grignard, B.; Gennen, S.; Jérôme, C.; Kleij, A. W.; Detrembleur, C. Advances in the use of CO_2 as a renewable feedstock for the synthesis of polymers. *Chem. Soc. Rev.* **2019**, *48*, 4466−4514.

(5) Ghosh, S.; Modak, A.; Samanta, A.; Kole, K.; Jana, S. *Mater. Adv.* **2021**, *2*, 3161−3187.

(6) Burkart, M. D.; Hazari, N.; Tway, C. L.; Zeitler, E. L. Opportunities and challenges for catalysis in carbon dioxide utilization. *ACS Catal.* **2019**, *9*, 7937.

(7) Dibenedetto, A.; Nocito, F. The future of carbon dioxide chemistry. *ChemSusChem* **2020**, *13*, 6219.

(8) Zhang, Z. E.; Pan, S. Y.; Li, H.; Cai, J. C.; Olabi, A. G.; Anthony, E. J.; Manovic, V. Recent advances in carbon dioxide utilization. *Renewable Sustainable Energy Rev.* **2020**, *125*, 109799.

(9) Hua, L. Y.; Li, B. X.; Han, C. P.; Gao, P. F.; Wang, Y. R.; Yuan, D.; Yao, Y. M. Synthesis of homo- and heteronuclear rare earth metal complexes stabilized by ethanolamine-bridged bis(phenolato) ligands and their application in catalyzing reactions of CO_2 and epoxides. *Inorg. Chem.* **2019**, *58*, 8775.

(10) Jin, L.; Huang, Y.; Jing, H.; Chang, T.; Yan, P. Chiral catalysts for the asymmetric cycloaddition of carbon dioxide with epoxides. *Tetrahedron: Asymmetry* **2008**, *19*, 1947−1953.

(11) Darensbourg, D. J.; Mackiewicz, R. M.; Phelps, A. L.; Billodeaux, D. R. Copolymerization of CO_2 and epoxides catalyzed by metal salen complexes. *Acc. Chem. Res.* **2004**, *37*, 836−844.

(12) Sit, W. N.; Ng, S. M.; Kwong, K. Y.; Lau, C. P. Coupling reactions of CO_2 with neat epoxides catalyzed by PPN salts to yield cyclic carbonates. *J. Org. Chem.* **2005**, *70*, 8583−8586.

(13) Paddock, R. L.; Nguyen, S. T. Chemical CO_2 fixation: Cr(III) salen complexes as highly efficient catalysts for the coupling of CO2 and epoxides. *J. Am. Chem. Soc.* **2001**, *123*, 11498−11499.

(14) Shaikh, R. R.; Pornpraprom, S.; D'Elia, V. Catalytic strategies for the cycloaddition of pure, diluted, and waste CO2 to epoxides under ambient conditions. *ACS Catal.* **2018**, *8*, 419−450.

(15) Büttner, H.; Longwitz, L.; Steinbauer, J.; Wulf, C.; Werner, T. Recent developments in the synthesis of cyclic carbonates from epoxides and CO_2. *Top. Curr. Chem.* **2017**, *375* (3), 375.

(16) Martín, C.; Fiorani, G.; Kleij, A. W. Recent advances in the catalytic preparation of cyclic organic carbonates. *ACS Catal.* **2015**, *5*, 1353−1370.

(17) Paddock, R. L.; Nguyen, S. T. Chiral (salen)Co^{III} catalyst for the synthesis of cyclic carbonates. *Chem. Commun.* **2004**, 1622.

(18) Miao, C. X.; Wang, J. Q.; Wu, Y.; Du, Y.; He, L. N. Bifunctional metal-salen complexes as efficient catalysts for the fixation of CO_2 with epoxides under solvent-free. *ChemSusChem* **2008**, *1*, 236.

(19) Paddock, R. L.; Nguyen, S. T. Chemical CO_2 fixation: Cr(III) salen complexes as highly efficient catalysts for the coupling of CO_2 and epoxides. *J. Am. Chem. Soc.* **2001**, *123*, 11498.

(20) Lu, X. B.; Liang, B.; Zhang, Y. J.; Tian, Y. Z.; Wang, Y. M.; Bai, C. X.; Wang, H.; Zhang, R. Asymmetric catalysis with CO_2: Direct synthesis of optically active propylene carbonate from racemic epoxides. *J. Am. Chem. Soc.* **2004**, *126*, 3732.

(21) Castro-Osma, J.; Lamb, K. J.; North, M. Cr(salophen) complex catalyzed cyclic carbonate synthesis at ambient temperature and pressure. *ACS Catal.* **2016**, *6*, 5012.

(22) Whiteoak, C. J.; Martin, E.; Escudero-Adán, E.; Kleij, A. W. Stereochemical divergence in the formation of organic carbonates derived from internal epoxides. *Adv. Synth. Catal.* **2013**, *355*, 2233.

(23) Della Monica, F.; Maity, B.; Pehl, T.; Buonerba, A.; Nisi, A. D.; Monari, M.; Grassi, A.; Rieger, B.; Cavallo, L.; Capacchione, C. [OSSO]-type iron(III) complexes for the lowpressure reaction of carbon dioxide with epoxides: catalytic activity, reaction kinetics, and computational study. *ACS Catal.* **2018**, *8*, 6882.

(24) Andrea, K. A.; Brown, T. R.; Murphy, J. N.; Jagota, D.; McKearney, D.; Kozak, C. M.; Kerton, F. M. *Inorg. Chem.* **2018**, *57*, 13494.

(25) Fazekas, E.; Nichol, G. S.; Shaver, M. P.; Garden, J. A. Stable Fe(III) phenoxyimines as selective and robust CO_2/epoxide coupling catalysts. *Dalton Trans.* **2018**, *47*, 13106.

(26) Della Monica, F.; Buonerba, A.; Paradiso, V.; Milione, S.; Grassi, A.; Capacchione, C. [OSSO]-type Fe(III) metallate as single-component catalyst for the CO_2 cycloaddition to epoxides. *Adv. Synth. Catal.* **2019**, *361*, 283.

(27) Seong, E. Y.; Kim, J. H.; Kim, N. H.; Ahn, K. H.; Kang, E. J. Multifunctional and sustainable Fe-iminopyridine complexes for the synthesis of cyclic carbonates. *ChemSusChem* **2019**, *12*, 409.

(28) Haak, R. M.; Decortes, A.; Escudero-Adán, E. C.; Belmonte, M. M.; Martin, E.; Benet-Buchholz, J.; Kleij, A. W. Shape-persistent octanuclear zinc salen clusters: synthesis, characterization, and catalysis. *Inorg. Chem.* **2011**, *50*, 7934.

(29) Decortes, A.; Belmonte, M. M.; Benet-Buchholza, J.; Kleij, A. W. Efficient carbonate synthesis under mild conditions through cyclo-addition of carbon dioxide to oxiranes using a Zn(salphen) catalyst. *Chem. Commun.* **2010**, *46*, 4580.

(30) Desens, W.; Kohrt, C.; Spannenberg, A.; Werner, T. A novel zinc based binary catalytic system for CO_2 utilization under mild conditions. *Org. Chem. Front.* **2016**, *3*, 156.

(31) Ma, R.; He, L. N.; Zhou, Y. B. An efficient and recyclable tetraoxo-coordinated zinc catalyst for the cycloaddition of epoxides with carbon dioxide at atmospheric pressure. *Green Chem.* **2016**, *18*, 226.

(32) Biswas, S.; Khatun, R.; Sengupta, M.; Islam, S. M. *Molecular Catalysis* **2018**, *452*, 129−137.

(33) Guo, Z. Q.; Xu, Y.; Chao, J. B.; Wei, X. H. Lithium organoaluminate complexes as catalysts for the conversion of CO_2 into cyclic carbonates. *Eur. J. Inorg. Chem.* **2020**, *2020*, 2835.

(34) Cozzolino, M.; Press, K.; Mazzeo, M.; Lamberti, M. Carbon dioxide/epoxide reactions catalyzed by bimetallic salalen aluminum complexes. *ChemCatChem.* **2016**, *8*, 455.

(35) Meléndez, D. O.; Lara-Sánchez, A.; Martínez, J.; Wu, X.; Otero, A.; Castro-Osma, J.; North, M.; Rojas, R. S. Amidinate aluminium complexes as catalysts for carbon dioxide fixation into cyclic carbonates. *ChemCatChem.* **2018**, *10*, 2271.

(36) Kim, Y.; Hyun, K.; Ahn, D.; Kim, R.; Park, M. H.; Kim, Y. *ChemSusChem* **2019**, *12*, 4211.

(37) Biswas, S.; Roy, D.; Ghosh, S.; Islam, S. M. *J. Organomet. Chem.* **2019**, *898*, 120877.

(38) Ema, T.; Miyazaki, Y.; Shimonishi, J.; Maeda, C.; Hasegawa, J. Y. Bifunctional porphyrin catalysts for the synthesis of cyclic carbonates from epoxides and CO_2: structural optimization and mechanistic study. *J. Am. Chem. Soc.* **2014**, *136*, 15270.

(39) Ema, T.; Miyazaki, Y.; Koyama, S.; Yano, Y.; Sakai, T. A bifunctional catalyst for carbon dioxide fixation: cooperative double activation of epoxides for the synthesis of cyclic carbonates. *Chem. Commun.* **2012**, *48*, 4489.

(40) Liu, X.; Zhang, S.; Song, Q. W.; Liu, X. F.; Ma, R.; He, L. N. Cooperative calcium-based catalysis with 1,8 diazabicyclo[5.4.0]-undec-7-ene for the cycloaddition of epoxides with CO_2 at atmospheric pressure. *Green Chem.* **2016**, *18*, 2871.

(41) Longwitz, L.; Steinbauer, J.; Spannenberg, A.; Werner, T. Calcium-based catalytic system for the synthesis of bio-derived cyclic carbonates under mild conditions. *ACS Catal.* **2018**, *8*, 665.

(42) Wang, L.; Zhang, G. Y.; Kodamaa, K.; Hirose, T. An efficient metal- and solvent-free organocatalytic system for chemical fixation of CO_2 into cyclic carbonates under mild conditions. *Green Chem.* **2016**, *18*, 1229.

(43) Sopeña, S.; Martin, E.; Escudero-Adán, E. C.; Kleij, A. W. Pushing the limits with squaramide-based organocatalysts in cyclic carbonate synthesis. *ACS Catal.* **2017**, *7*, 3532.

(44) Liu, N.; Xie, Y. F.; Wang, C.; Li, S. J.; Wei, D. H.; Li, M.; Dai, B. Cooperative multifunctional organocatalysts for ambient conversion of carbon dioxide into cyclic carbonates. *ACS Catal.* **2018**, *8*, 9945.

(45) Hu, J. Y.; Ma, J.; Liu, H. Z.; Qian, Q. L.; Xie, C.; Han, B. X. Dual-ionic liquid system: an efficient catalyst for chemical fixation of CO_2 to cyclic carbonates under mild conditions. *Green Chem.* **2018**, *20*, 2990.

(46) Wu, X.; Chen, C. T.; Guo, Z. Y.; North, M.; Whitwood, A. C. *ACS Catal.* **2019**, *9*, 1895.

(47) Hao, Y. H.; Yuan, D.; Yao, Y. M. Metal-free cycloaddition of epoxides and carbon dioxide catalyzed by triazole-bridged bisphenol. *ChemCatChem.* **2020**, *12*, 4346.

(48) Pineda, E. M.; Lan, Y.; Fuhr, O.; Wernsdorfer, W.; Ruben, M. Exchange-bias quantum tunnelling in a CO_2-based Dy_4-single molecule magnet. *Chem. Sci.* **2017**, *8*, 1178−1185.

(49) Pineda, E. M.; Lorusso, G.; Zangana, K. H.; Palacios, E.; Schnack, J.; Evangelisti, M.; Winpenny, R. E. P.; McInnes, E. J. L. Observation of the influence of dipolar and spin frustration effects on the magneto-caloric properties of a trigonal prismatic $\{Gd_7\}$ molecular nanomagnet. *Chem. Sci.* **2016**, *7*, 4891−4895.

(50) Ugale, B.; Dhankhar, S. S.; Nagaraja, C. M. Exceptionally stable and 20-connected lanthanide metal-organic frameworks for selective CO_2 capture and conversion at atmospheric pressure. *Cryst. Growth Des.* **2018**, *18*, 2432−2440.

(51) Xue, Z.; Jiang, J.; Ma, M. G.; Li, M. F.; Mu, T. Gadolinium-based metal-organic framework as an efficient and heterogeneous catalyst to activate epoxides for cycloaddition of CO_2 and alcoholysis. *ACS Sustainable Chem. Eng.* **2017**, *5*, 2623−2631.

(52) Wei, N.; Zuo, R. X.; Zhang, Y. Y.; Han, Z. B.; Gu, X. J. Robust high-connected rare-earth MOFs as efficient heterogeneous catalysts for CO_2 conversion. *Chem. Commun.* **2017**, *53*, 3224−3227.

(53) Li, Y.; Zhang, X.; Lan, J.; Li, D.; Wang, Z.; Xu, P.; Sun, J. A high-performance zinc-organic framework with accessible open metal sites catalyzes CO_2 and styrene oxide into styrene carbonate under mild conditions. *ACS Sustainable Chem. Eng.* **2021**, *9*, 2795−2803.

(54) Chen, H.; Fan, L.; Zhang, X. Nanoporous Zn^{II}/Tb^{III}-organic frameworks for CO_2 conversion. *ACS Appl. Nano Mater.* **2020**, *3*, 7201−7210.

(55) Moreno-Pineda, E.; Wernsdorfer, W. Measuring molecular magnets for quantum technologies. *Nature Reviews* **2021**, *3* (9), 645−659.

(56) Moreno-Pineda, E.; Godfrin, C.; Balestro, F.; Wernsdorfer, W.; Ruben, M. Molecular spin qudits for quantum algorithms. *Chem. Soc. Rev.* **2018**, *47*, 501−513.

(57) Tang, J.; Zhang, P. *In Lanthanide Single Molecule Magnets*; Springer: Berlin Heidelberg, 2015; Vol. 2, pp 41−90.

(58) Long, J. Luminescent Schiff-Base Lanthanide Single-Molecule Magnets: The Association Between Optical and Magnetic Properties. *Front. Chem.* **2019**, *7*, 00063.

(59) Quahab, L., Ed. *Multifunctional Molecular Materials*; Pan Stanford Publishing: Singapore, 2013.

(60) Wang, J.; Zakrzewski, J. J.; Heczko, M.; Zychowicz, M.; Nakagawa, K.; Nakabayashi, K.; Sieklucka, B.; Chorazy, S.; Ohkoshi, S.-i. Proton Conductive Luminescent Thermometer Based on Near-Infrared Emissive $\{YbCo_2\}$ Molecular Nanomagnets. *J. Am. Chem. Soc.* **2020**, *142*, 3970−3979.

(61) Furukawa, T.; Miyagawa, K.; Taniguchi, H.; Kato, R.; Kanoda, K. Quantum criticality of Mott transition in organic materials. *Nat. Phys.* **2015**, *11*, 221.

(62) Ferrando-Soria, J.; Khajavi, H.; Serra-Crespo, P.; Gascon, J.; Kapteijn, F.; Julve, M.; Lloret, F.; Pasán, J.; Ruiz-Pérez, C.; Journaux, Y.; Pardo, E. Highly Selective Chemical Sensing in a Luminescent Nanoporous Magnet. *Adv. Mater.* **2012**, *24*, 5625−5629.

(63) Karachousos-Spiliotakopoulos, K.; Tangoulis, V.; Panagiotou, N.; Tasiopoulos, A.; Moreno-Pineda, E.; Wernsdorfer, W.; Schulze, M.; Botas, A. M. P.; Carlos, L. D. Luminescence thermometry and field induced slow magnetic relaxation based on a near infrared emissive heterometallic complex. *Dalton Trans.* **2022**, *51*, 8208−8216.

(64) Biswas, S.; Das, S.; Rogez, G.; Chandrasekhar, V. Hydrazone-Ligand-Based Homodinuclear Lanthanide Complexes: Synthesis, Structure, and Magnetism. *Eur. J. Inorg. Chem.* **2016**, *2016* (20), 3322−3329.

(65) Dolai, M.; Moreno-Pineda, E.; Wernsdorfer, W.; Ali, M.; Ghosh, A. Exchange-Bias Quantum Tunneling of the Magnetization in a Dysprosium Dimer. *J. Phys. Chem. A* **2021**, *125*, 8230−8237.

(66) Yu, W.; Schramm, F.; Moreno Pineda, E.; Lan, Y.; Fuhr, O.; Chen, J.; Isshiki, H.; Wernsdorfer, W.; Wulfhekel, W.; Ruben, M. Single-molecule magnet behavior in 2,2′-bipyrimidine-bridged dilanthanide complexes. *Beilstein journal of nanotechnology* **2016**, *7*, 126−137.

(67) Moreno Pineda, E.; Taran, G.; Wernsdorfer, W.; Ruben, M. Quantum tunnelling of the magnetisation in single-molecule magnet isotopologue dimmers. *Chemical science* **2019**, *10* (19), 5138−5145.

(68) Lindh, R.; et al. OpenMolcas: From Source Code to Insight. *J. Chem. Theory Comput.* **2019**, *15* (11), 5925−5964.

(69) Lines, M. E. Orbital Angular Momentum in the Theory of Paramagnetic Clusters. *J. Chem. Phys.* **1971**, *55*, 2977.

(70) Moreno Pineda, E.; Chilton, N. F.; Marx, R.; Dörfel, M.; Sells, D. O.; Neugebauer, P.; Jiang, S.-D.; Collison, D.; van Slageren, J.; McInnes, E. J.L.; Winpenny, R. E. P. Direct measurement of dysprosium(III)dysprosium(III) interactions in a single-molecule magnet. *Nat. Commun.* **2014**, *5* (1), 5243.

(71) Ghosh, A. K.; Saha, U.; Biswas, S.; ALOthman, Z. A.; Islam, M. A.; Dolai, M. Anthracene-triazole-dicarboxylate-Based Zn(II) 2D Metal Organic Frameworks for Efficient Catalytic Carbon Dioxide Fixation into Cyclic Carbonates under Solvent-Free Condition and Theoretical Study for the Reaction Mechanism. *Ind. Eng. Chem. Res.* **2022**, *61*, 175.

(72) Lan, J.; Qu, Y.; Zhang, X.; Ma, H.; Xu, P.; Sun, J. A novel water-stable MOF Zn(Py)(Atz) as heterogeneous catalyst for chemicalconversion of CO_2 with various epoxides under mild conditions. *J. CO2 Util.* **2020**, *35*, 216−224.

(73) Xu, C.; Liu, Y.; Wang, L.; Ma, J.; Yang, L.; Pan, F.; Kirillovc, A. M.; Liu, W. *Dalton Trans.* **2017**, *46*, 16426−16431.

(74) Hua, L.; Li, B.; Han, C.; Gao, P.; Wang, Y.; Yuan, D.; Yao, Y. *Inorg. Chem.* **2019**, *58*, 8775−8786.

(75) Xin, X.; Shan, H.; Tian, T.; Wang, Y.; Yuan, D.; You, H.; Yao, Y. *ACS Sustainable Chem. Eng.* **2020**, *8*, 13185−13194.

(76) Hou, W.; Wang, G.; Wu, X.; Sun, S.; Zhao, C.; Liu, W.-S.; Pan, F. *New J. Chem.* **2020**, *44*, 5019−5022.

(77) Dhankhar, S. S.; Nagaraja, C. M. *New J. Chem.* **2020**, *44*, 9090−9096.

(78) Sinchow, M.; Semakul, N.; Konno, T.; Rujiwatra, A. *ACS Sustainable Chem. Eng.* **2021**, *9*, 8581−8591.

(79) Cheng, J.; Lu, C.; Zhao, B. *New J. Chem.* **2021**, *45*, 13096−13103.

(80) Chen, C.; Zhang, A. *New J. Chem.* **2021**, *45*, 20155−20163.